

Comparison between holographic and transient-photocurrent measurements of electron mobility in photorefractive $\text{Bi}_{12}\text{SiO}_{20}$

J. P. Partanen, P. Nouchi, J.M.C. Jonathan, * and R.W. Hellwarth

Department of Electrical Engineering and Department of Physics, University of Southern California, Los Angeles, California 90089-0484

(Received 1 October 1990; revised manuscript received 7 February 1991)

We have developed a time-of-flight technique for measuring the mobility of photoexcited charge carriers in certain crystals exhibiting the electro-optic effect. We used this holographic technique to find that the mobility of photoexcited electrons in a previously well-characterized sample of *n*-type $\text{Bi}_{12}\text{SiO}_{20}$ is $0.24 \pm 0.07 \text{ cm}^2 \text{ V}^{-1} \text{ s}^{-1}$, independent of electric field in our range of observation ($\approx 200\text{--}2000 \text{ V/cm}$). We also present results of transient photocurrent measurements. When used with our absorption measurement and previously reported values of the quantum efficiency and mobility-lifetime product, they give two independent estimates of electron mobility that are consistent with our directly measured value.

I. INTRODUCTION

The mobility of photoexcited carriers in photorefractive insulating crystals is a key parameter in determining the response time of a material. However, its reliable measurement has proven to be more difficult than expected. In nominally undoped $\text{Bi}_{12}\text{SiO}_{20}$ previous measurements using purely electrical experimental techniques have provided conflicting values ranging from $5 \times 10^{-5} \text{ cm}^2 \text{ V}^{-1} \text{ s}^{-1}$ to $3 \text{ cm}^2 \text{ V}^{-1} \text{ s}^{-1}$.¹⁻⁴ Similarly conflicting values have been reported for structurally similar $\text{Bi}_{12}\text{GeO}_{20}$.^{2,4} The measurements of Refs. 1 and 2 are based on the transit time of photoexcited carriers through a thin sample, but they do not show the usual top-hat profile⁵ of photocurrent, which is easy to analyze. Instead, shapes of current pulses lead to concepts like "dispersive" phototransport⁶ for which, strictly speaking, the mobility cannot be defined. The mobility values quoted in Refs. 3 and 4 are based on the absolute magnitude of the photocurrent combined with measurements of the optical absorption coefficient and estimates of quantum efficiency (fraction of absorbed photons creating photo-carriers), thus giving only qualitative estimates of the mobility. Purely electrical mobility measurements also suffer from complications caused by electrode potentials, surface currents, and nonuniform electric fields, which can even change during the course of the measurement.

Optical measurements of the range (or diffusion length) of photoexcited charge carriers⁷ have also been used to estimate the charge-carrier mobilities of $\text{Bi}_{12}\text{SiO}_{20}$ and $\text{Bi}_{12}\text{GeO}_{20}$. The diffusion length is proportional to the square root of the mobility and the lifetime of the photoexcited carriers. By measuring the lifetime and using the diffusion length measurement of Ref. 7, Le Saux, Launey, and Brun⁸ inferred a mobility of $130 \text{ cm}^2 \text{ V}^{-1} \text{ s}^{-1}$ for carriers in $\text{Bi}_{12}\text{GeO}_{20}$. Jonathan, Rossignol, and Roosen⁹ measured the build-up time of the photorefractive grating excited by picosecond pulses in $\text{Bi}_{12}\text{SiO}_{20}$ and deduced the value $50 \text{ cm}^2 \text{ V}^{-1} \text{ s}^{-1}$ for the carrier mobility. Another optical determination of the charge-carrier mobility

was performed by Astratov, Il'inskii, and Furman.¹⁰ They studied the growth of electrical screening field through the electro-optic effect and evaluated values from 10^{-9} to $10^{-4} \text{ cm}^2 \text{ V}^{-1} \text{ s}^{-1}$ at temperatures from 130 to 200 K, respectively. At higher temperatures the screening field development was too complicated for the determination of mobility.¹¹

Here we report a direct holographic time-of-flight measurement of a photoexcited charge-carrier mobility in an insulator.¹² We find the electron mobility to be $0.24 \pm 0.07 \text{ cm}^2 \text{ V}^{-1} \text{ s}^{-1}$ in a previously well-characterized sample of $\text{Bi}_{12}\text{SiO}_{20}$. We also report transient photocurrent measurements from which we obtain two independent estimates of this mobility, (1) using the absolute value of photocurrent, as in Refs. 3 and 4 ($0.13 \pm 0.08 \text{ cm}^2 \text{ V}^{-1} \text{ s}^{-1}$), and (2) using the recombination time, as in Ref. 8 ($0.17 \pm 0.1 \text{ cm}^2 \text{ V}^{-1} \text{ s}^{-1}$). These two qualitative estimates from photocurrent experiments are consistent with our holographic measurement of mobility. In the time-of-flight mobility measurement we use the spatially sinusoidal intensity pattern of overlapping picosecond laser pulses to excite a sinusoidal pattern of electrons into the conduction band, where it drifts under the influence of a strong applied static electric field. The spatially modulated space-charge field caused by the excited electrons and the ions they leave behind is initially zero, grows to a maximum after electrons have moved one-half of the period of the intensity pattern, and fall to a minimum after the full period. We probe the space-charge field with a Bragg-matched cw laser through the electro-optic effect. The electron drift velocity and thus the mobility are calculated from the time required for electrons to drift one period. Pauliat *et al.*¹³ recently used a similar kind of method to measure the mobility in $\text{Bi}_{12}\text{GeO}_{20}$, however, with cw laser excitation and an alternating applied electric field.

We present a simple theory for our holographic time-of-flight technique in Sec. II. Because estimates for mobility and lifetime of photoexcited charge carriers from photocurrent experiments were required to set experi-

mental conditions suitable for the time-of-flight mobility measurement, we describe the transient photocurrent measurements in Sec. III before describing the holographic mobility measurement in Sec. IV. In Sec. V we discuss some implications of the small value of the mobility (compared to drift mobilities in semiconductors), which we measured.

II. THEORY OF HOLOGRAPHIC TIME-OF-FLIGHT TECHNIQUE

We assume that the photorefractive crystal is illuminated with two short interfering laser pulses that are negligibly attenuated, resulting in an energy flux distribution inside the crystal given by (in units of J cm^{-2})

$$U(z) = U_0 [1 + \text{Re}(me^{ikz})] . \quad (1)$$

Here m is the modulation depth and k is the wave vector of the interference pattern. The laser pulse is considered to be so short that the excited charge carriers may be assumed not to move noticeably in space during the pulse. We will assume that after the excitation, the movement of electrons is described (in the dark) by the following four equations. (Similar equations for holes may be constructed when needed.¹⁴) First we assume that the ionized donor density $N_D^+(z, t)$ changes only by the single direct recombination process:

$$\frac{\partial N_D^+}{\partial t} = -\gamma N_D^+ n . \quad (2)$$

Here γ is the recombination rate constant. Then, the continuity equation for the density $n(z, t)$ of photoexcited electrons is

$$\frac{\partial n}{\partial t} = \frac{1}{e} \frac{\partial j}{\partial z} - \gamma N_D^+ n , \quad (3)$$

where e is the (positive) charge of the electron. The current density $j(z, t)$ is assumed to consist only of a drift and a diffusion z component near thermal equilibrium at temperature T , so that it can be written in the form

$$j = e\mu nE + \mu k_B T \frac{\partial n}{\partial z} , \quad (4)$$

where μ is the (positive) electron mobility and k_B is Boltzmann's constant. Finally, the Poisson equation for the superposition $E(z, t)$ of Coulomb fields arising from the charged donor density N_D^+ and excited electron density n is, in SI (Système International) units

$$\frac{\partial E}{\partial z} = \frac{e}{\epsilon} (N_D^+ - N_A - n) , \quad (5)$$

where ϵ is the dielectric constant and the constant N_A is the density of acceptor sites required to make the crystal electrically neutral in the dark at static equilibrium. At low excitation energy fluxes the initial values of N_D^+ , n and E can be written in the same form as the energy flux of (1). Because we consider only the case of small modulation $|m| \ll 1$, we only need to keep terms that are constant in space or that vary as e^{ikz} at subsequent times:

$$\begin{aligned} N_D^+(t, z) &= N_0(t) + \text{Re}[N_1(t)e^{ikz}] , \\ n(t, z) &= n_0(t) + \text{Re}[n_1(t)e^{ikz}] , \\ E(t, z) &= E_0(t) + \text{Re}[E_1(t)e^{ikz}] . \end{aligned} \quad (6)$$

Although we may quote parameters in other units, the formulas here will always be assumed to be in SI units.

We will assume that the laser-pulse energy flux U_0 is small enough so that n_0 and n_1 are proportional to U_0 . Substituting (6) in (2)–(5) shows that this requires first that $n_0 \ll N_A$, so that N_D^+ can be replaced by N_A ($\approx 10^{16} \text{ cm}^{-3}$) in the right-hand side of (2). More stringently, it requires the average density of excited electrons to be much smaller than the saturation density n_s defined by

$$n_s = \frac{\gamma N_A \epsilon}{\mu e} + k^2 \frac{k_B T \epsilon}{e^2} , \quad (7)$$

so that we only need to keep terms in (3) that are linear in U_0 . In our experiments k^2 is much less than K_e^2 ($\equiv \gamma N_A e / \mu k_B T$), which was found to be $3 \times 10^6 \text{ cm}^{-2}$ in Ref. 14. This gives $n_s \geq 10^{12} \text{ cm}^{-3}$. With these approximations (3) and (4) give

$$\frac{\partial n_1}{\partial t} = - \left[\gamma N_A + k^2 \mu \frac{k_B T}{e} - ik\mu E_0 \right] n_1 , \quad (8)$$

which can be solved immediately. With the same assumptions we get an equation for E_1 :

$$\frac{\partial E_1}{\partial t} = \frac{e}{\epsilon} \left[\mu E_0 + ik\mu \frac{k_B T}{e} \right] n_1 . \quad (9)$$

With the solution for n_1 from (8) we find a solution to (9):

$$E_1(t) = E_\infty (1 - e^{-\Gamma t}) , \quad (10)$$

which satisfies the initial condition $E_1(0) = 0$, and in which

$$\Gamma \equiv \Gamma' + i\Gamma'' = \gamma N_A + k^2 \mu \frac{k_B T}{e} - ik\mu E_0 \quad (11)$$

and

$$E_\infty = -\mu \frac{e}{\epsilon} n_1(0) \frac{E_0 + ikk_B T/e}{\Gamma} . \quad (12)$$

It is clear from (11) that the imaginary part Γ'' of the damping constant does not depend on any other material parameters than the mobility itself. If the experimental conditions are arranged to be such that Γ'' is larger than Γ' , the temporal oscillation in the amplitude E_1 of the grating electric field becomes visible and the mobility μ can be determined from the oscillation period, i.e., the time it takes for an electron to drift one grating period. From (5) the oscillation is caused by the superposition of the stationary ionic grating upon the grating of electrons drifting with constant velocity under the influence of the strong and applied electric field E_0 , with the two space-charge fields canceling each other initially, and at each subsequent time when the gratings coincide. The requirement that Γ'' be clearly larger than Γ' corresponds to the requirement that photoexcited carriers drift at least one

period before experiencing recombination and significant effects from diffusion.

We observe the time development of the space-charge field grating by diffracting a laser beam from it. The diffraction efficiency η is proportional to the square of the amplitude E_1 of the Coulomb grating, so the time behavior of η is, from (10),

$$\eta = \eta_\infty |1 - e^{-(\Gamma' + i\Gamma'')t}|^2, \quad (13)$$

where η_∞ is the value of diffraction efficiency after the oscillations have damped out.

III. TRANSIENT PHOTOCURRENT EXPERIMENTS

We studied photoexcited carriers in a $5 \times 5 \times 5$ mm³ *n*-type Bi₁₂SiO₂₀ single crystal grown by Sumitomo and designated as crystal SU1 in Ref. 14, where it was characterized by fitting quasi-cw two-beam coupling and grating erasure data to the electron-hole competition model. These experiments did not determine the mobility μ and the recombination time τ separately, but only their product. Therefore we first made the following photocurrent measurements to obtain estimates of μ and τ separately, and to predict a useful grating spacing for the time-of-flight measurement.

We studied the decay of the photocurrent induced in the crystal by a uniformly illuminating 30-ps laser pulse when an electric field (≈ 1 kV/cm) was applied to the crystal, which is coated with two conducting electrodes separated by d . At low fluences (≤ 30 $\mu\text{J}/\text{cm}^2$) the decay of the photocurrent $i(t)$ can be fit by two exponential decays over several orders of magnitude in time and level of signal (as reported in Ref. 3). The time constants for the exponential decays are $t_1 = 26 \pm 3$ ns and $t_2 = 80 \pm 5$ μs . The faster component displaced about 1% of the charge of the slower one. A convenient way to present the photocurrent data is to express it in the form of the average magnitude $x_a(t)$ of the distance traveled by a photoexcited charge carrier:

$$x_a(t) = N^{-1} \sum_{n=1}^N |x_n(t)| = \frac{d}{Ne} \int_0^t i(t') dt' \quad (14)$$

and plot the curves using logarithmic scales. Here $x_n(t)$ is the distance traveled by the n th carrier in the direction of the electric field, and N is the total number of mobile carriers generated by the laser pulse. We estimate N by applying the observation of Ref. 14 that nearly every absorbed photon excites a carrier to our measured absorption coefficient of 0.74 ± 0.25 cm⁻¹. Taking into account the 20% Fresnel reflection at each surface of the crystal, we find the $\ln(x_a)$ vs $\ln(t)$ curve shown in Fig. 1 with the two characteristic shoulders corresponding to the two different exponential decays. The parameters of the two exponentials are consistent with the predictions that one would make assuming the electron-hole model and the parameters of Ref. 14 for SU1, if we take, in addition, the hole and electron recombination times to be, respectively, the t_1 and t_2 of Fig. 1. However, *any* reasonable model would have to associate the longer t_2 with the electrons that are clearly the majority carriers for the photorefractive effect, and the majority contributors for $x_a(\infty)$ in

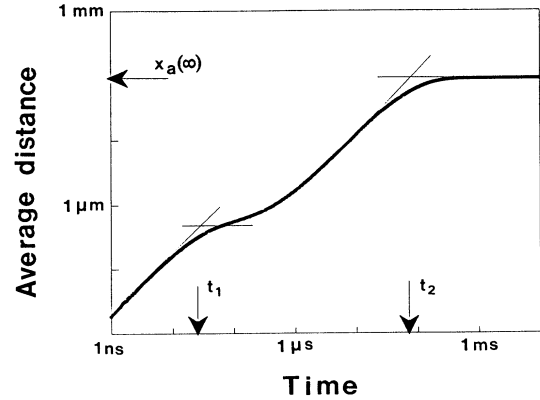


FIG. 1. Average distance $x_a(t)$ traveled by photoexcited charge carriers as a function of time t , calculated by Eq. (14) from our photocurrent measurements at low fluences (≤ 30 $\mu\text{J}/\text{cm}^2$) and at average applied electric field of 1 kV/cm.

Fig. 1. We see that the majority carriers (electrons) travel about 100 μm , before recombination when the applied electric field is of the order of 1 kV/cm. Therefore we adjust the grating period to be about 100 μm in the experiments of the next section.

We can determine a preliminary value for the electron mobility [$\mu_a = x_a(t)/(E_0 t)$] from Fig. 1. Using values for x_a and t just before the second shoulder and taking into account the quantum efficiency of 0.86 for electron excitation¹⁴ we get $\mu = 0.13 \pm 0.08$ cm² V⁻¹ s⁻¹. As was mentioned in the Introduction, another, independent estimate of mobility uses the recombination time $t_2 = 80 \pm 5$ μs measured here and diffusion length $K_d^{-1} = 5.8 \pm 2.3$ μm reported in Ref. 14 for electrons in the same sample. This gives a value $\mu = 0.17 \pm 0.1$ cm² V⁻¹ s⁻¹.

IV. HOLOGRAPHIC TIME-OF-FLIGHT MOBILITY EXPERIMENT

Our holographic time-of-flight mobility measurement employs the experimental arrangement illustrated in Fig. 2. The interference pattern is written by 30-ps frequency-doubled pulses (at 5 Hz) from a Nd/YAG (yttrium aluminum garnet) laser at the wavelength of 532 nm. The beam expander (BE) creates uniform illumination of the sample. The beam splitter BS1 provides two beams S_1 and S_2 . Beam S_1 illuminates a Ronchi ruling R which is imaged on the Bi₁₂SiO₂₀ sample by a pair of Fourier-transforming lenses L_1 and L_2 . In the intermediate Fourier plane an aperture A selects the two lowest-order components (0 and -1 or 1) diffracted by R . The crystal is thus illuminated by a sinusoidal distribution of intensity whose period is 93 μm and modulation depth $|m|$ is near 1. The writing pulse energy flux was 1 $\mu\text{J}/\text{cm}^2$ ($n_0 \approx 1.6 \times 10^{12}$ cm⁻³). Beam S_2 is used to erase the previously written gratings by uniformly illuminating the crystal from the back. Two electronically controlled shutters Sh_1 and Sh_2 ensure single-pulse writing of the grating and its erasure. A voltage V_0 is applied to the crystal by a power supply which is electronically switched on just before the writing pulse to minimize

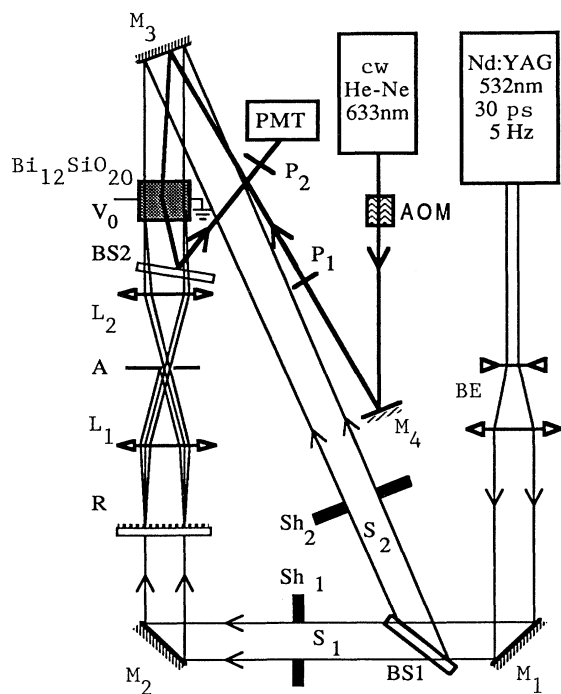


FIG. 2. Experimental arrangement for time-of-flight measurement of mobility of electrons in sample $\text{Bi}_{12}\text{SiO}_{20}$.

space-charge field buildup. The crystal is oriented so that the grating wave vector is along its (110) crystallographic axis. The diffraction efficiency is monitored using a $10\text{-}\mu\text{W}$ He-Ne laser beam that is linearly polarized by P_1 so that the polarization of the light scattered by defects in the crystal is largely orthogonal to that of the diffracted beam and can be blocked by the polarizer P_2 . An acousto-optic modulator (AOM) is used to turn the He-Ne beam on synchronously with the writing pulse from the Nd/YAG laser, and turn it off during the erasure phase. A careful timing allows full decay of the space-charge field between successive writing pulses and minimizes the effect of the photocurrents produced by the He-Ne beam, which is switched on only $200\text{ }\mu\text{s}$ before the writing pulses. A photomultiplier tube (PMT) measures the time evolution of the diffracted signal. The noisy signal is averaged over about 50 shots and filtered both electronically at the input of the storage digital oscilloscope and later numerically. The total integration time of this smoothing process is kept smaller than 0.1 times the time interval between the laser pulse and the diffraction maximum.

Figure 3 shows the experimental time evolution of the diffraction efficiency for SU1 with the voltage $V_0 = 1\text{ kV}$ applied across the crystal, along with the best fit of this data to (13) having η_∞ , Γ' , and Γ'' as fitting parameters. To be able to evaluate the mobility from (13) we must know the value of the applied electric field E_0 inside the crystal. It has been frequently observed that E_0 inside photorefractive materials does not generally equal V_0/d , where d is the distance between the electrodes.¹⁵ We measured the electric field E_0 in a separate experiment

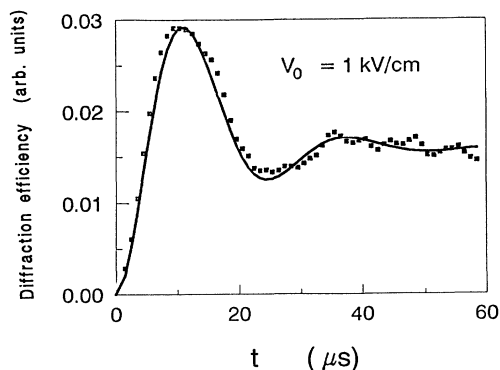


FIG. 3. Time behavior of diffraction efficiency in $\text{Bi}_{12}\text{SiO}_{20}$ sample after picosecond photoexcitation pulse. The solid curve is a plot of Eq. (13) with $\Gamma' = 8.6 \times 10^4\text{ s}^{-1}$ and $\Gamma'' = 2.42 \times 10^5\text{ s}^{-1}$, which gives the least mean-squares error when compared to data.

using the change in the polarization of the transmitted He-Ne beam caused by the electro-optic effect and using the analysis of Ref. 15. The values measured for E_0 were typically $0.7 V_0/d$, with the coefficient increasing slightly with V_0 . To characterize the uniformity of E_0 across the crystal these measurements were done with a beam diameter of 0.4 mm , one-third of the beam size used for the diffraction experiment. The field E_0 was found to be uniform within 5% both along and normal to the electric-field direction. We also could observe that E_0 did not change more than 5% during the buildup of the photorefractive grating.

The imaginary part Γ'' of the parameter in (11) divided by k is the mean electron drift velocity \bar{v} . A plot of the drift velocity \bar{v} , obtained from best-fit Γ'' values as a function of E_0 is shown in Fig. 4, demonstrating linear variation and confirming that the photoconduction is Ohmic. From this set of data we obtain a mobility $\mu = 0.24\text{ cm}^2\text{ V}^{-1}\text{ s}^{-1}$ with the main uncertainty arising from the uncertainty in the average electric field, which we estimate could be as far off from our electro-optic measurement as is V_0/d ($\approx \pm 30\%$). We also found that, contrary to (11), the best-fitting Γ' also varies linearly

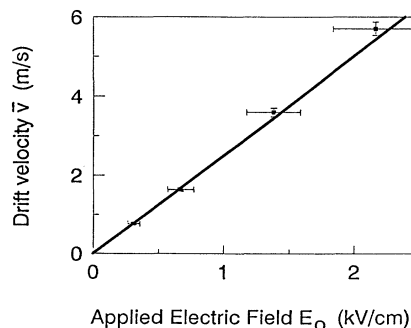


FIG. 4. Mean electron drift velocity \bar{v} vs applied electric field E_0 as determined by fitting Eq. (13) to four curves, such as shown in Fig. 3. $\bar{v} \equiv \Gamma''/k$.

with the electric field E_0 for points of Fig. 4. We have shown that this is consistent with a random variation of mobility ($\pm 40\%$) across the crystal volume.¹²

V. DISCUSSION

The electron mean free path, calculated from the standard expression $[\mu(2k_B T m)^{1/2}/e]$ and our measured $\mu = 0.24 \text{ cm}^2 \text{ V}^{-1} \text{ s}^{-1}$, is less than the typical separation of atoms in the crystal lattice. This indicates that the model of collision-limited free-electron transport in the conduction band does not apply to the photoexcited electrons that we are observing. However, our measurements demonstrate that the average drift velocity depends linearly on the applied electric field (Fig. 4) and therefore justifies the concept of mobility. Our low mobility value can be explained as a trap-limited mobility μ_t .¹⁶ Photoexcited electrons do not move in the conduction band continuously. They fall occasionally to an energy level from which they can be thermally excited. The trap-limited mobility is related to the actual conduction-band mobility μ_c by the expression

$$\mu_t = \mu_c \frac{\tau_t}{\tau_t + \tau_r}, \quad (15)$$

where τ_t is the average time spent by a conduction electron between trapping events and τ_r is the average time for a trapped electron before its release. Shallow-trap models have already been used in analyses of charge transport in photorefractive materials.^{2-4,10,17}

The wide range of mobility values reported in the literature may also be an indication of trap-limited trans-

port processes: small differences (greater than $k_B T$) in the depths of traps can indeed lead to an order-of-magnitude difference in thermal excitation rates and thus in trap-limited mobilities. By their nature, shallow-trap events are always dominated by a very narrow energy interval in the gap.¹⁶

In conclusion, we demonstrate here how a holographic method can be used to measure mobilities of photoexcited charge carriers in photorefractive materials. Using this method on a well-characterized *n*-type $\text{Bi}_{12}\text{SiO}_{20}$ crystal we found a mobility of $0.24 \pm 0.07 \text{ cm}^2 \text{ V}^{-1} \text{ s}^{-1}$ for the electrons. The conductivity caused by these photoexcited electrons was found to be Ohmic over our experimental range of 200–2000 V/cm in the electric field. We also estimated electron mobility values indirectly by two independent ways from transient photocurrent measurements reported here and from previous holographic characterization of the same sample. We found good agreement among all three mobility values.

ACKNOWLEDGMENTS

We want to acknowledge helpful discussions with Dr. M. B. Klein and Dr. R. A. Mullen. This research was supported by the U.S. Air Force Office of Scientific Research, under Contract No. F 49620-88-C-0027, and by the National Science Foundation, under Grant No. ECS-8821507. The Institut d'Optique is "Unité associée au Centre National de la Recherche Scientifique No. 14."

*Permanent address: Institut d'Optique, Boîte Postale 147, 91403, Orsay, France.

¹S. L. Hou, R. B. Lauer, and R. E. Aldrich, *J. Appl. Phys.* **44**, 2652 (1973).

²B. Kh. Kostyuk, A. Yu. Kudzin, and G. Kh. Sokolyanskii, *Fiz. Tverd. Tela (Leningrad)* **22**, 2454 (1980) [*Sov. Phys.—Solid State* **22**, 1429 (1980)].

³G. Le Saux and A. Brun, *IEEE J. Quantum Electron.* **QE-23**, 1680 (1987).

⁴I. T. Ovchinnikov and E. V. Yanshin, *Fiz. Tverd. Tela (Leningrad)* **25**, 2196 (1983) [*Sov. Phys.—Solid State* **25**, 1265 (1983)].

⁵R. G. Kepler, *Phys. Rev.* **119**, 1226 (1960).

⁶H. Scher and E. W. Montroll, *Phys. Rev. B* **12**, 2455 (1975); G. Pfister and H. Scher, *ibid.* **15**, 2062 (1977).

⁷R. A. Mullen and R. W. Hellwarth, *J. Appl. Phys.* **58**, 40 (1985).

⁸G. Le Saux, J. C. Launay, and A. Brun, *Opt. Commun.* **57**, 166 (1986).

⁹J. C. M. Jonathan, Ph. Rossignol, and G. Roosen, *Opt. Lett.* **13**, 224 (1988).

¹⁰V. N. Astratov, A. V. Il'inskii, and A. S. Furman, *Pis'ma Zh. Tekh. Fiz.* **14**, 1330 (1988) [*Sov. Tech. Phys. Lett.* **14**, 581 (1988)].

¹¹V. N. Astratov, A. V. Il'inskii, and V. A. Kiselev, *Fiz. Tverd. Tela (Leningrad)* **26**, 2843 (1984) [*Sov. Phys.—Solid State* **26**, 1720 (1984)].

¹²J. P. Partanen, J. M. C. Jonathan, and R. W. Hellwarth, *Appl. Phys. Lett.* **57**, 2404 (1990).

¹³G. Pauliat, A. Villing, J. C. Launay, and G. Roosen, *J. Opt. Soc. Am. B* **7**, 1481 (1990).

¹⁴F. P. Strohkendl, P. Tayebati, and R. W. Hellwarth, *J. Appl. Phys.* **66**, 6024 (1989).

¹⁵J. M. C. Jonathan, R. W. Hellwarth, and G. Roosen, *IEEE J. Quantum Electron.* **QE-22**, 1936 (1986).

¹⁶*Photoconductivity and Related Phenomena*, edited by J. Mort and D. M. Pai (Elsevier, Amsterdam, 1976).

¹⁷G. Pauliat and G. Roosen, *J. Opt. Soc. Am. B* **7**, 2259 (1990).